Available online at www.sciencedirect.com
ScienceDirect
International Journal of Mass Spectrometry 272 (2008) 119–126
International Journal of Mass Spectrometry
www.elsevier.com/locate/ijms

Electron interaction with S_6-$C_{60}(CF_3)_{12}$: Energy pool of fullerene cage

Rustem V. Khatymov [a], Vitaliy Yu. Markov [b], Renat F. Tuktarov [a], Ilya N. Ioffe [b], Mars V. Muftakhov [a], Stanislav M. Avdoshenko [b], Andrey V. Pogulay [a], Lev N. Sidorov [b,*]

[a] *Institute of Molecular and Crystal Physics, Ufa Research Center, Russian Academy of Sciences, Oktyabrya av. 151, 450075 Ufa, Russia*
[b] *Chemistry Department, Moscow State University, Leninskiye gory 1-3, 119991 Moscow, Russia*

Received 15 December 2007; received in revised form 18 January 2008; accepted 23 January 2008
Available online 6 February 2008

Abstract

Electron impact study of isomer S_6-$C_{60}(CF_3)_{12}$ resulted in the ionization efficiency curves (IEC) of singly and doubly charged positive ions and electron capture resonances for negative ones. The appearance energy (AE) values of the fragment $C_{60}(CF_3)_n$ ions appear to correlate linearly with n down to $n=0$ (C_{60} ion) and its value for each additional act of CF_3 detachment rises by 2–3 eV. Observations of metastable ions reveal several cases of quasi-simultaneous detachment of two CF_3-groups. Energy shift between ionization energy of S_6-$C_{60}(CF_3)_{12}$ and AE of the first fragment $C_{60}(CF_3)_{11}$ ion was observed as 8.8 eV for singly and 8.3 eV for doubly charged ions. To rationalize this energy shift a DFT calculation of the orbital energies for the $C_{60}(CF_3)_{12}^+$ cation have been carried out and energy gap between HOMO and LUMO orbitals was estimated. High probability of occupation of the localized σ* orbital and CF_3-elimination require four electron excitation and can be effected via a multielectron transition from the multitude of the densely distributed occupied π orbitals. The analogies with the fragmentation of C_{60} with C_2-elimination are mentioned.

Keywords: Fullerene; $C_{60}(CF_3)_{12}$; Appearance energy; Fragmentation

1. Introduction

Among various intriguing properties of C_{60} is its remarkable stability under electron impact conditions. It is commonly accepted today that the dominant fragmentation pathway involves sequential loss of C_2 units with appearance threshold of the C_{58} cation around 30–40 eV (i.e. at least two times higher than the sum of the ionization energy, 7.57 ± 0.01 eV, and the activation energy for fragmentation), further fragmentation thresholds being spaced by almost regular intervals of 5.0–5.6 eV [1–3]. Certain decrease of the first threshold for the ions with longer timeframe of formation clearly indicated the kinetic nature of the exaggerated energy demands [1]. These observations have been rationalized in [1–3] with the use of the quasi-thermodynamic Rice–Ramsperger–Kassel–Marcus (RRKM) and finite heat bath (FHB) [4] models with an implicit assumption of equilibrium distribution of excitation energy.

Among the tremendous amount of available fullerene derivatives, most suitable for gas-phase studies are fluorinated and trifluoromethylated molecules that can be thermally desorbed without decomposition. Analogously to the aforementioned phenomena, the difference in appearance energy (AE) values between the molecular ($C_{60}F_{18}^+$, $AE = 8.1 \pm 1.0$ eV), and the first fragment ion ($C_{60}F_{17}^+$, 16.3 ± 0.9 eV) exceeded the C–F bond energy more than twice [5]. Similarly, the AE values of the $C_{60}(CF_3)_n^+$ ions with odd n were 6–8 eV higher than those of ions with even n [6].

An important feature of fullerene molecules that has to be mentioned in the context of discussion of ionization behavior is relatively high cross-section of multielectron excitation. Such processes, which can be due to strong electronic correlation within the shell of π orbitals, have been extensively described for pristine C_{60}, where they can be excited both optically [7,8] and collisionally (including the electron capture processes) [9–11] and are usually referred to as surface plasmon resonance peaked between 15 and 25 eV, as can be traced by energy dependence of single- and multiphoton ionization and fragmentation [7,8].

Recently the first selective synthesis and X-ray crystallographic study of S_6-$C_{60}(CF_3)_{12}$ has been reported [12]. High

* Corresponding author. Tel.: +7 095 9391240; fax: +7 095 9391240.
E-mail address: sidorov@phys.chem.msu.ru (L.N. Sidorov).

1387-3806/$ – see front matter © 2008 Elsevier B.V. All rights reserved.
doi:10.1016/j.ijms.2008.01.007

isomeric purity, known structure and availability of the temperature dependence of saturated vapor pressure [13] make this compound the excellent object to expand the studies of interaction of fullerene molecules with electrons. In this paper we report electron impact ionization and electron capture studies of S_6-$C_{60}(CF_3)_{12}$.

2. Experimental

2.1. Sample preparation

The sample of S_6-$C_{60}(CF_3)_{12}$ was manufactured according to the known procedure [12]. C_{60} was heated with CF_3I at 440 °C for 2 days in a sealed double-sectioned glass ampoule, the CF_3I section kept at ambient temperature. The admixtures to the poorly soluble S_6-$C_{60}(CF_3)_{12}$ were washed several times with toluene and subsequently with 1,2-dichlorobenzene. Crystalline S_6-$C_{60}(CF_3)_{12}$ is insoluble in these solvents, whereas all other known trifluoromethylfullerenes are soluble (see details in Ref. [14]). The sample was characterized by X-ray powder diffraction and IR-spectroscopy which demonstrated its complete identity with the literature data [12]. Therefore, the purity of the sample can be estimated as 99+%. The mass spectra of MALDI and EI showed trace of $C_{60}(CF_3)_{10}$ and $C_{60}(CF_3)_{14}$ admixtures in some probes of the sample. It can be accounted for by the presence of small inclusions in crystalline S_6-$C_{60}(CF_3)_{12}$ occurring during a crystal growth.

2.2. Electron ionization (EI) and electronic capture (EC) mass spectrometry

The mass spectrometric apparatus was based on the modified MI-1201V magnetic sector device capable to acquire EI and EC mass spectra and energy curves [15]. The scheme of the apparatus is shown in Fig. 1.

Briefly, the electrons emitted from a tungsten cathode (electron current 1–10 μA) and collimated by the field of the focusing electromagnet ($B \approx 100$ G) interact with the vapor molecules in the ionization chamber. The FWHM of the electron energy dispersion was estimated to be 0.3–0.5 eV on the basis of the effective yield curve (EYC) of the SF_6^- ion from SF_6 (maximum at ca. 0 eV). The ions thus formed are accelerated and mass analyzed by a sector magnetic analyzer. Measurements of the ionization efficiency curves (IEC) for the positive ions (EI mode) or the effective yield curves for negative ions (EC mode) can be performed in the electron energy range of 0–80 eV. To calibrate the electron energy in the EI mode, the AE values of Ar^+ and Ar^{2+} ions [16] were used for the singly and doubly charged ions, respectively, while the maximum of the effective yield curve of SF_6^- ion from SF_6 was used as a calibration reference in the EC mode. The measured total pressure in the ionization region was below 10^{-5} Pa, which ensures the desired single collision regime of electron–molecule interactions. In order to increase the ion signal, the sample was placed directly in the temperature-controlled ionization chamber heated to 165–180 °C.

2.3. Matrix-assisted laser desorption/ionization (MALDI) mass spectrometry

To make a comparison of different techniques, the ionization processes of S_6-$C_{60}(CF_3)_{12}$ were also studied under the MALDI conditions. In this purpose we applied Bruker AutoFlex II reflectron time-of-flight mass spectrometer (Germany) equipped with N_2 laser (337 nm, 1 ns pulse duration). Its control system was able to operate in the post-source

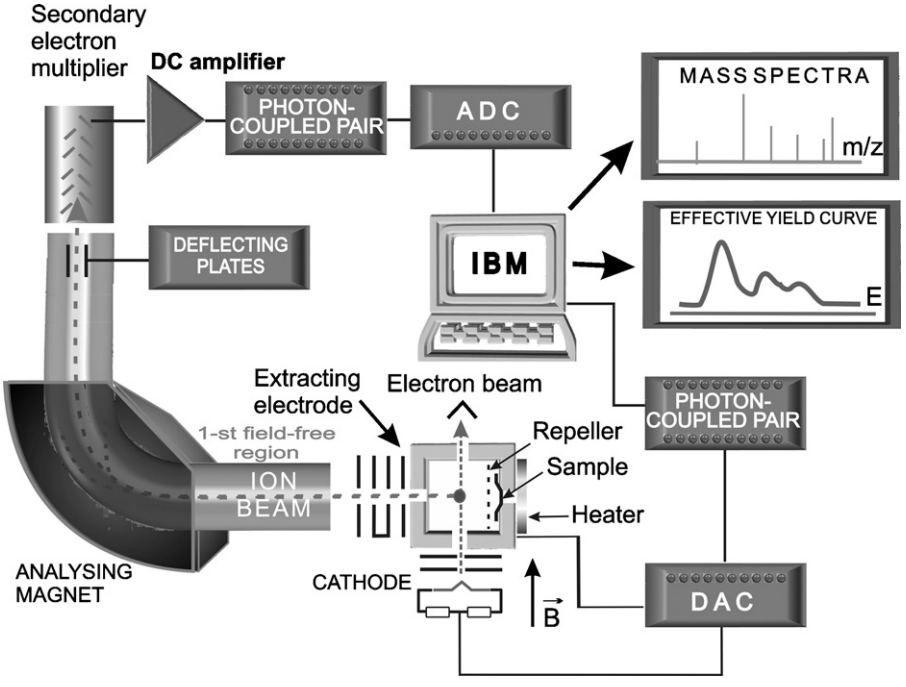

Fig. 1. The block diagram of the mass spectrometric system applied to record EI and EC mass spectra.

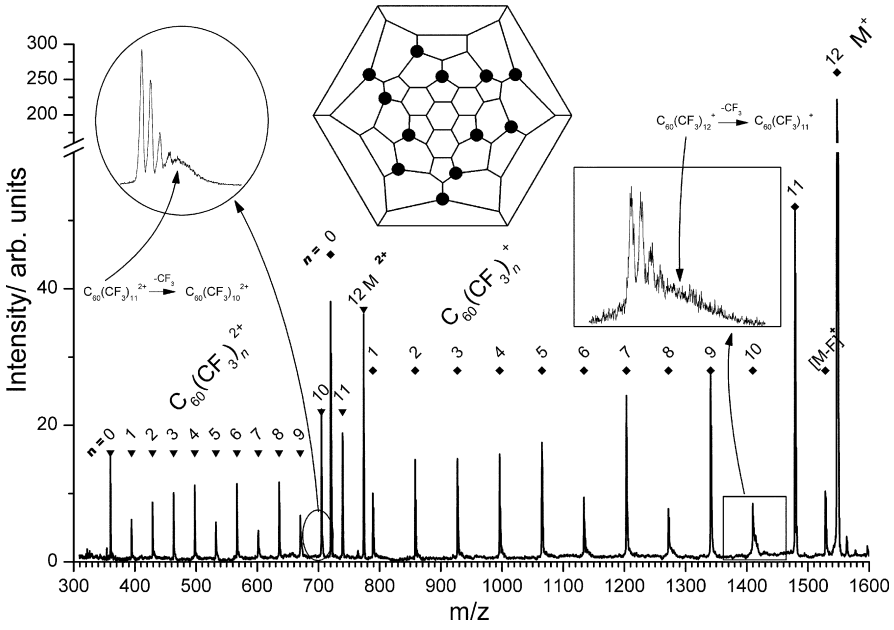

Fig. 2. The EI mass spectrum of S_6-$C_{60}(CF_3)_{12}$, electron energy 70 eV. Insets demonstrate the metastable peaks due to CF_3-group loss by single- and double-charged ions and the chemical structure of S_6-$C_{60}(CF_3)_{12}$ as a Schlegel diagram from [12] (double bonds are not distinguished). In marks: squares, single-charged peaks; triangles, double-charged peaks; circles, CF_3-groups in a Schlegel diagram and $M = C_{60}(CF_3)_{12}$.

decay (PSD) mode [17]. *Trans*-2-[3-(4-*tert*-butylphenyl)-2-methyl-2-propenylidene]malononitrile (DCTB) {≥ 99%, Fluka, Switzerland} was used as a matrix.

3. Results

3.1. EI mass spectra and IEC

EI mass spectra of S_6-$C_{60}(CF_3)_{12}$ (see Fig. 2) consist of $C_{60}(CF_3)_n^+$ and $C_{60}(CF_3)_n^{2+}$ signals with $n = 0$–12, their ratios depending on the electron energy. Figs. 3 and 4 present the ionization efficiency curves for some singly and doubly charged ions, respectively. The AE values (see Table 1) were derived from IEC by a weighted, non-linear least-squares fitting pro-

Table 1
Appearance energies (AE) for single-charged $C_{60}(CF_3)_n^+$ and double-charged $C_{60}(CF_3)_n^{2+}$ ions with $n = 0$–12 ions from the EI mass spectrum of S_6-$C_{60}(CF_3)_{12}$

n	AE {$C_{60}(CF_3)_n^+$} (eV)	AE {$C_{60}(CF_3)_n^{2+}$} (eV)
12	8.7 ± 0.4	21.7 ± 0.5
11	17.5 ± 0.9	30.0 ± 0.4
10[a]	9.4 ± 1.4, 20.8 ± 1.1	32.4 ± 0.3
9	22.8 ± 1.3	34.3 ± 0.7
8	25.3 ± 1.2	36.7 ± 0.5
7	27.9 ± 0.9	39.5 ± 0.6
6	30.3 ± 1.1	41.5 ± 0.5
5	33.1 ± 0.7	43.9 ± 0.7
4	35.6 ± 0.9	46.1 ± 0.5
3	38.2 ± 1.1	48.3 ± 0.8
2	41.6 ± 0.9	51.2 ± 0.6
1	44.3 ± 1.2	53.3 ± 1.0
0	46.8 ± 1.2	56.4 ± 1.6

[a] Two ionization thresholds for single-charged $C_{60}(CF_3)_{10}^+$ (see Fig. 3).

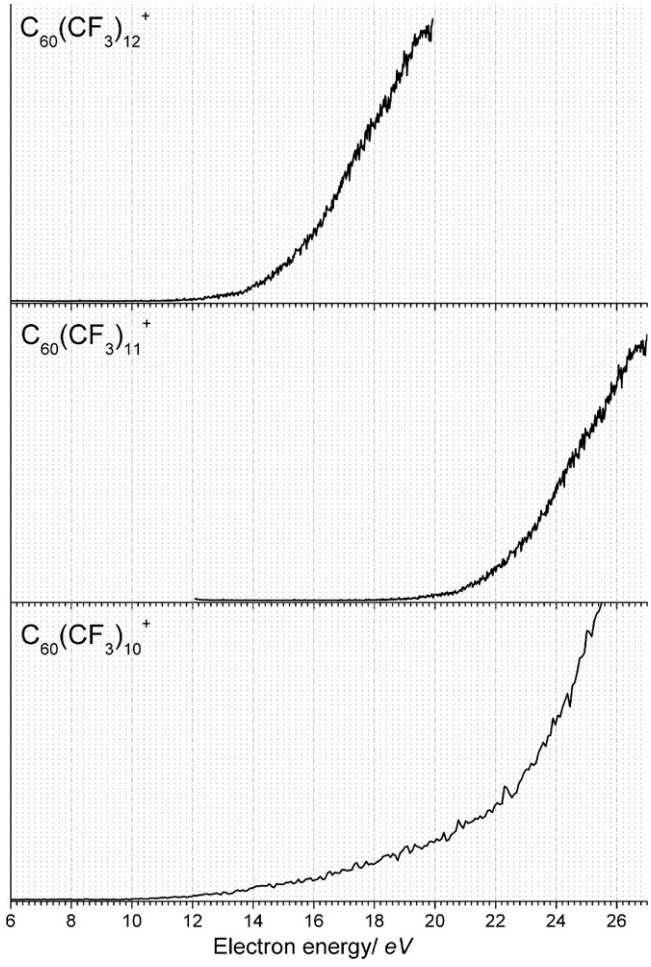

Fig. 3. IEC for single-charged $C_{60}(CF_3)_n^+$ ions with $n = 10$–12 from the EI mass spectrum of S_6-$C_{60}(CF_3)_{12}$.

cedure using the Marquardt–Levenberg algorithm. The weights were chosen as $1/(N+1)$ where N is the total number of counts per energy bin. For curves with one ionization threshold the fitting function was taken from work [18]. In the case of two thresholds we used the modified function described in [19].

The AE values of $C_{60}(CF_3)_n^+$ with $n=10$ (first threshold) and 12 singly charged ions appeared to be close to the ionization energies of molecules of fullerenes and their derivatives [1–6]. Therefore, these ions originate from the corresponding molecules. For $C_{60}(CF_3)_n^+$ with $n=0$–9 and 11 AE values are considerably higher and unambiguously indicate in their fragment nature. However, IEC of $C_{60}(CF_3)_{10}^+$ shows the second threshold at 20.8 ± 1.1 eV (see Fig. 3) likely to be due to the fragment contribution. The AE values of the fragment $C_{60}(CF_3)_n^+$ ions (including the second threshold for $n=10$) appear to correlate linearly with n down to $n=0$ (C_{60}^+ ion), as depicted in Fig. 5. Similar correlation can be found for the $C_{60}(CF_3)_n^{2+}$ doubly charged fragment ions. In general, the AE value for each additional act of CF_3 detachment rises by 2–3 eV. In addition to the stable peaks, the mass spectrum (see insets in Fig. 2) also includes some metastable signals due to abstraction of a single CF_3-group:

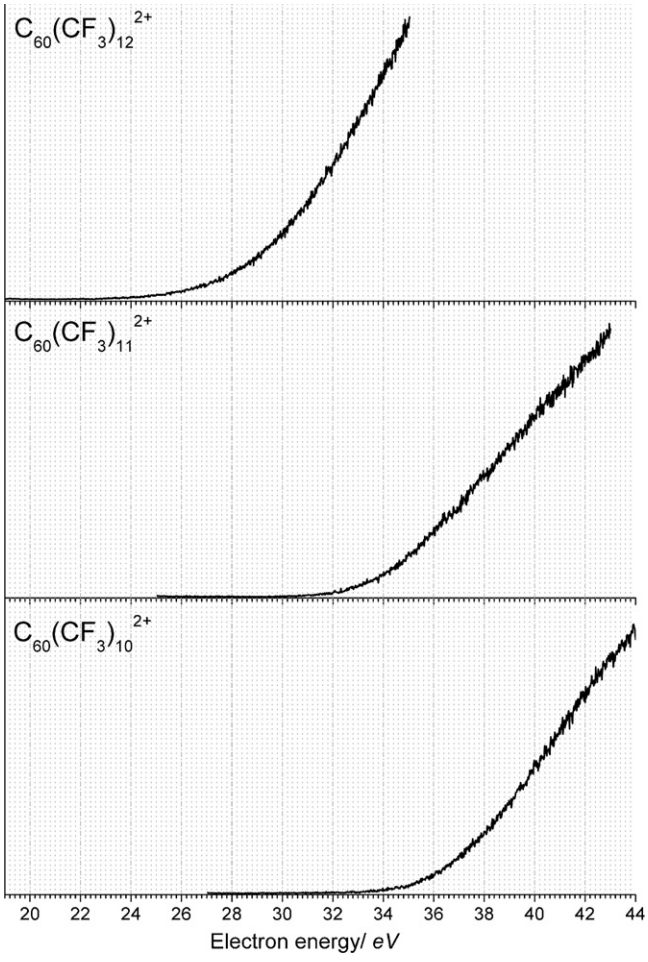

Fig. 4. IEC for double-charged $C_{60}(CF_3)_n^{2+}$ ions with $n=10$–12 from the EI mass spectrum of S_6-$C_{60}(CF_3)_{12}$.

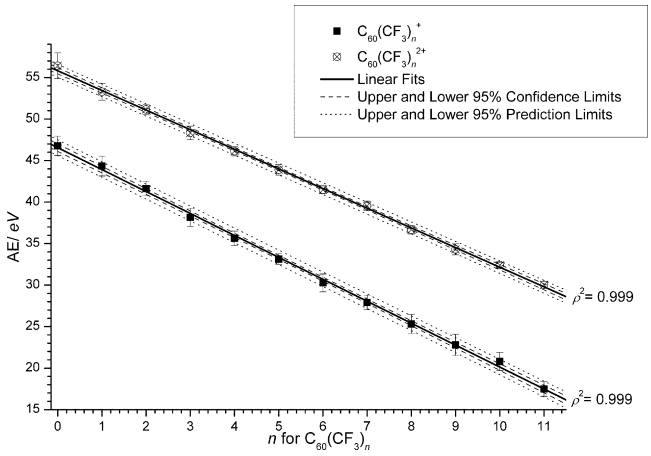

Fig. 5. The plots (experimental points, linear fits, confidence and prediction limits) of AE values for $C_{60}(CF_3)_n^+$ and $C_{60}(CF_3)_n^{2+}$ ions vs. n, $n=0$–11. The values of correlation coefficient squares are inserted.

$$C_{60}(CF_3)_n^+ \rightarrow C_{60}(CF_3)_{n-1}^+ + CF_3, \qquad n = 1\text{–}12,$$
$$C_{60}(CF_3)_n^{2+} \rightarrow C_{60}(CF_3)_{n-1}^{2+} + CF_3, \qquad n = 1\text{–}12.$$

3.2. EC mass spectra and EYC

Fig. 6 depicts EYC for $C_{60}(CF_3)_n^-$ ions, $n=0$–12, from the EC mass spectrum of S_6-$C_{60}(CF_3)_{12}$. In an agreement with the EI data, only the EYC of $C_{60}(CF_3)_n^-$ with $n=10$, 12 exhibit zero-energy resonances near indicative of their molecular nature, the EYC of $C_{60}(CF_3)_{10}^-$ additionally containing the second peak ca. 11 eV higher due to detachment of two CF_3-groups from $C_{60}(CF_3)_{12}^-$. Due to the mixed $C_{60}(CF_3)_{12}$ and $C_{60}(CF_3)_{10}$ origins, the $C_{60}(CF_3)_n^-$ ions with $n=2$–9 also give rise to at least two peaks or shoulders. Taking into consideration only $C_{60}(CF_3)_{12}$-based peaks (see attributions in EYC of Fig. 6), which are generally more intense with the exception of $C_{60}(CF_3)_{10}^-$, $C_{60}(CF_3)_8^-$ and $C_{60}(CF_3)_6^-$, one can note gradual increase of the peak energy by 2–4 eV per each detached CF_3-group.

3.3. MALDI mass spectra

In Fig. 7 we present the positive and negative ion MALDI mass spectra of S_6-$C_{60}(CF_3)_{12}$. According to the PSD spectra (see insets in Fig. 7), the main fragmentation channel under the MALDI conditions is associated, analogously to the above described cases, with abstraction of the variable number of CF_3-groups. Noteworthy, a trend is observable that the formation of closed-shell fragments, namely ions with the odd number of CF_3-groups and even number of electrons, is somewhat favored.

4. Discussion

Of 17.5 eV AE value 8.7 eV are allocated to the ionization of the parent $C_{60}(CF_3)_{12}$. Correspondingly, 8.8 eV are required to effect the detachment of the first CF_3-group (and a very sim-

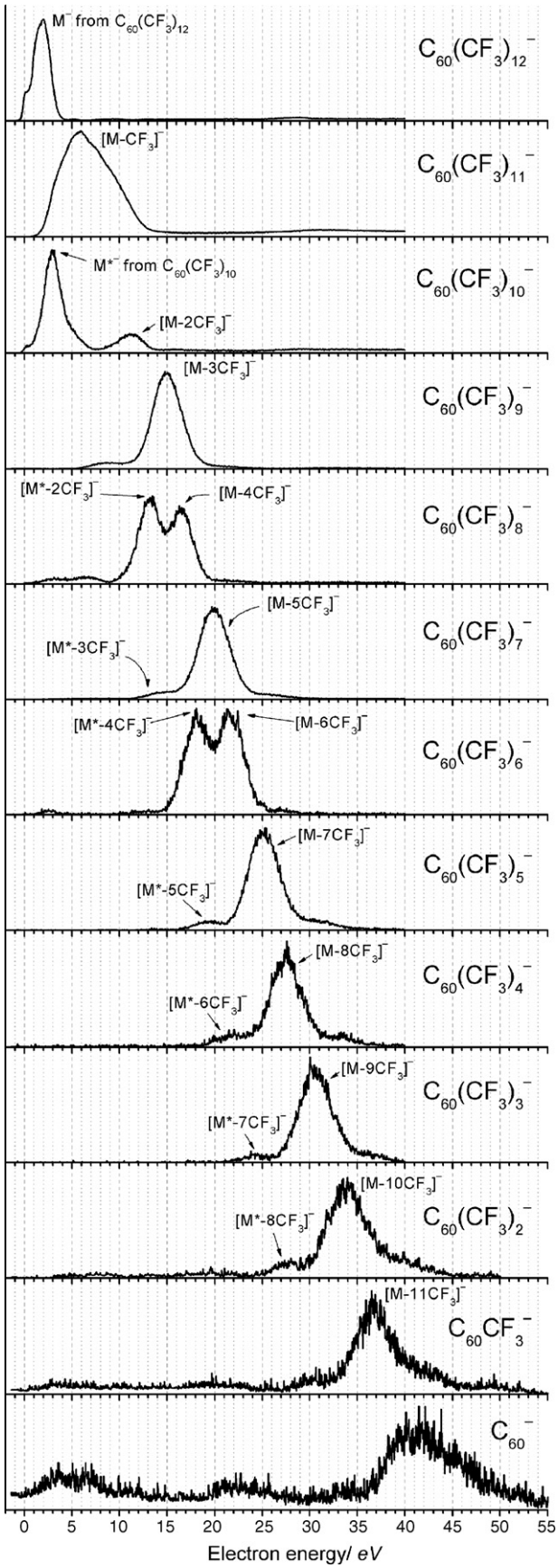

Fig. 6. EYC for $C_{60}(CF_3)_n^-$ ions, $n = 0$–12, from EC mass spectrum of S_6-$C_{60}(CF_3)_{12}$, energy range 0–55 eV. In marks: $M = C_{60}(CF_3)_{12}$; $M^* = C_{60}(CF_3)_{10}$.

ilar value of 8.3 eV is observed for the doubly charged ions), whereas, according to our DFT calculations, the dissociation energy of the C–CF_3 bond does not exceed 3.0 eV at most and 2.5 eV on average. Thus, the analogies with the fragmentation of C_{60} are again apparent [1–3].

Although it is quite likely that the reported case is analogous to the case of C_{60} in having quasi-thermodynamic roots, we did like to consider the exaggerated energy demands $C_{60}(CF_3)_{12}$ from a slightly different, though closely related, viewpoint. To rationalize our experimental results, a DFT (PBE/TZ2P) calculation (PRIRODA package [20]) of the orbital energies for the $C_{60}(CF_3)_{12}^+$ cation have been carried out. According to the comparison with the ultraviolet (UV) [21] photoelectron and near-edge X-ray absorption fine structure (NEXAFS) spectra, this theoretical methodology provides sufficiently accurate qualitative description of the frontier orbitals in fullerene derivatives. The calculated spectra of the α- and β-spin orbitals of cation are shown in Fig. 8. The unoccupied orbitals (except for the lowest, ionized one) appear to be a mixture of π* contributions of the unsaturated fragments and the σ* contributions of the C–CF_3 bonds.

Originally, we came to an impression that the more pronounced σ* contributions can be observed only in the orbitals starting 2.4 eV above the ground state while the four orbitals between 2.2 and 2.4 eV are of clearer π* nature. As an act of detachment of a CF_3-group requires either an extremely high-localized vibrational excitation, or an electronic excitation to a σ* orbital, the presence of the closely located π* states can considerably decrease the dissociation probability by providing a relaxation channel for the σ* states via vibronic coupling. Consequently, partial or complete population of the said π* orbitals can be expected to increase the dissociation rate. The said population can be effected via a multielectron transition from the multitude of the densely distributed occupied π orbitals of ground state. Once the four π* orbitals of a positive ion are populated, excitation of each additional electron will populate an orbital with a sound σ* contribution and will be thus likely to result in detachment of an additional CF_3-group. In other words, it was hypothesized that the said four π* orbitals act as a sort of a buffer reservoir to be filled. Indeed, the detachment threshold for the first CF_3-group is close to the sum of ionization energy and excitation energy for four electrons, as estimated from the orbital spectrum, whereas the portions of energy that cause the subsequent acts of detachment are close to the amount required for excitation of an extra electron (sufficiently dense spectrum of both occupied and unoccupied frontier orbitals can give rise to a large number of excitations of comparable energy).

More detailed analysis of the LUMO orbitals has, however, demonstrated that the ratio of π* and σ* contributions is quite comparable for all those LUMOs mentioned above. Therefore, an explanation of more general nature has to be suggested. Typically, detachment of a CF_3 group requires excitation of an electron from a bonding σ(C–CF_3) orbital to an antibonding σ*(C–CF_3) orbital. Our DFT analysis (PBE/TZ2P) has demonstrated that in $C_{60}(CF_3)_{12}$ the said orbitals are delocalized and mixed with the dense groups of the π-HOMOs and the π*-LUMOs, respectively, the same remaining true for the molecular

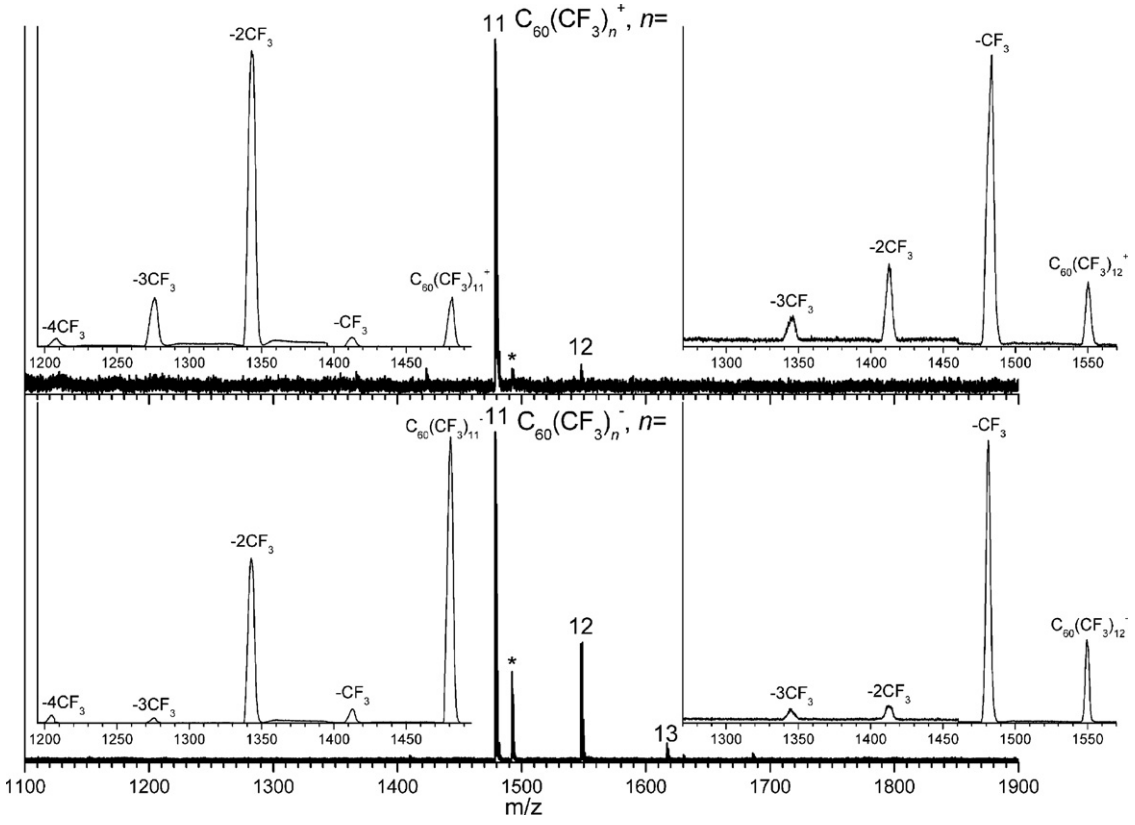

Fig. 7. The MALDI mass spectra (DCTB matrix) of positive (top) and negative (bottom) ions for S_6-$C_{60}(CF_3)_{12}$, the metastable peaks marked with *. Insets are the PSD spectra of $C_{60}(CF_3)_{11}^+$ (top on the left), $C_{60}(CF_3)_{12}^+$ (top on the right), $C_{60}(CF_3)_{11}^-$ (bottom on the left) and $C_{60}(CF_3)_{12}^-$ (bottom on the right).

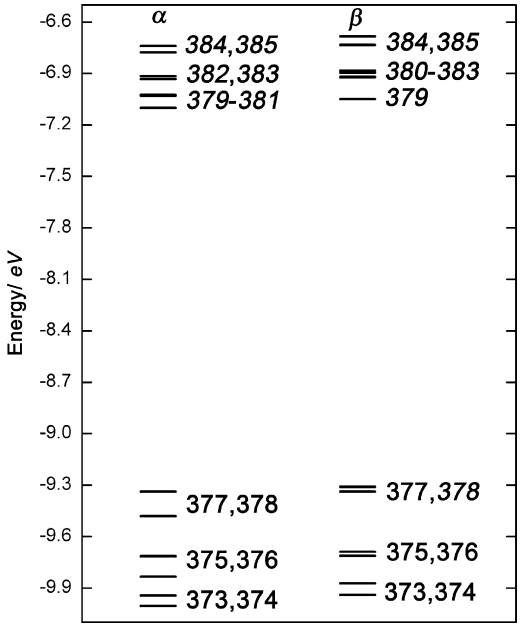

Fig. 8. Molecular α- and β-spin orbitals diagram of the $C_{60}(CF_3)_{12}^+$ cation according to the DFT (PBE/TZ2P) calculation. Occupied orbitals are numbered with regular type, vacant orbitals with italics. The orbitals below the gap represent a mixture of the σ and π contributions, while the orbitals above the gap comprise σ^* and π^* contributions.

ions. Hence of decisive importance may be multielectron shake-ups to the said $\sigma^* + \pi^*$ delocalized LUMOs that can retain similarity with collective electron excitation treated as the surface plasmon resonance in pristine C_{60}. Although there is hardly any possibility of precise estimation of multielectron excitation energy in a molecule that large, it may be not coincidental that the lowest estimated single electron excitation energies in $C_{60}(CF_3)_{12}$ are, according to our DFT calculations, pretty close to the experimentally measured appearance energy gaps between the successive fragments (2.3 eV), except for the above-discussed 8.8 eV (about four excitation energies) required for the first fragment, $C_{60}(CF_3)_{11}^+$.

The electrons excited to the above-mentioned LUMOs of the mixed nature will likely be delocalized not only within one given orbital but also within a broader group of them due to close location and, perhaps, intersections of potential energy surfaces, electronic correlation, and energy distribution in an ion ensemble measured. Detachment of a CF_3-group requires, on the contrary, localization of antibonding electron density on the respective C–CF_3 bond. However, only upon a pronounced stretching of the said bond there expectedly occurs, according to our DFT data, gradual segregation of a localized σ^* orbital accompanied by the decrease of its energy. Since the stretched configurations are of quite low probability in the equilibrium or near-equilibrium vibrational ensemble, the rate of fragmentation is likely to be relatively low. However, this rate will obviously increase with the number of electrons excited to the LUMOs due to their higher integral σ^* antibonding contribution and,

accordingly, higher probability of occupation of the localized σ* orbital when it emerges. If a given number of excited electrons are enough to reach the dissociation threshold, additional excitation will be likely to increase the dissociation rate considerably and thus provide a sufficient number of precursors for the next dissociation stage. The first stage, i.e. formation of $C_{60}(CF_3)_{11}^+$ is likely to require, as suggested by the threshold observed, four electron excitation. It is currently not known, whether this estimate depends on the experimental timeframe and sensitivity or is of more fundamental nature due to competition with some finitely small probability of radiative decay; the ICR-MS experiments might prove helpful here. The considerable abundance of metastable ions detected may serve as an indirect evidence that dissociation of ions is not completed within the 0.1 μs experimental window.

Interestingly, observations of metastable ions reveal several cases of quasi-simultaneous detachment of two CF_3-groups. This may be due to 0.7–1.0 eV lower detachment energy values in those cases when the original ion is opened-shell and the detachment product is closed-shell, as observed in our DFT calculations. As a result, detachment of a CF_3-group from an initially closed-shell ion may be followed by a much faster second act detachment returning the ion into the closed-shell state. This agrees with the preferable formation of closed-shell species during the post-source decay of MALDI-generated ions (see Fig. 7). The peak energies of the negative ions in the EC mass spectra appear to demonstrate subsequent elimination of CF_3-groups and analogous regular separation by 3.0 ± 0.8 eV (see peaks due to parent $C_{60}(CF_3)_{12}$ molecule in Fig. 6), i.e. slightly higher than the C–CF_3 bond energy.

It can be hypothesized that similar considerations can be applicable to the case of C_{60} too. However, an important distinction is apparent: the LUMOs of C_{60} are of pure π* nature, whereas the σ* orbitals of C–C bonds are located somewhat higher. Accordingly, to prevent rapid radiationless decay of the relevant σ* states into the nearby π* ones, it may be necessary to fill the π* orbitals by means of a multielectron transition. Moreover, the number of σ*(C–C) orbitals to be populated in order to effect dissociation may be even higher than in the case of $C_{60}(CF_3)_{12}$, as simultaneous dissociation of four C–C bonds that bind any C_2 fragment in C_{60} will require much higher activation energy. Therefore, much higher fragmentation threshold of C_{60} is hardly surprising.

One can note an interesting coincidence that for the quite similar timeframes of the C_{60} and the $C_{60}(CF_3)_{12}$ experiments the ratio of the threshold fragment energy to the activation energy of dissociation is close to the same value of 4 in both cases. It might be interesting to investigate whether the said value may be common to other fullerene derivatives of comparable size.

5. Conclusion

The observations of this paper and their interpretation may be conveniently illustrated by a mechanical analogy of a barrel tightly secured in a shallow pit and being filled by a high-pressure stream of water. The walls of the barrel provide a barrier for leaking, which would otherwise become energetically favorable upon filling above the pit level. However, the kinetic energy of the stream would transform in quite perturbed motion of water; as a result, some leaking over the walls will occur well before the complete filling and will increase with the amount of water filled in. In the reported case of $C_{60}(CF_3)_{12}$, the said amount of water represents the energy of the colliding electron, the pit level corresponds to the dissociation energy, the capacity of the barrel symbolizes the electronic degrees of freedom effectively coupled to the desired dissociative state, and "leaking" proceeds via detachment of the CF_3-groups, the easiest-to-detach fragments, and, of course, via ionization. Unfortunately, the analogy is not perfect, as the detachment of fragments is, unlike leaking, a discrete process. Besides, it should be taken into account that the characteristic time of radiative cooling of an isolated ion may be higher than the experimental timeframe available.

Our $C_{60}(CF_3)_{12}$ "barrel" has been observed to consume about 8.7 eV above the ionization demands to reach the ionization threshold within the experimental interval of 10^{-5} s. This is roughly four times higher than the characteristic C_{60}-CF_3 dissociation energy (the "pit level"). Almost equidistant separation of the further fragmentation thresholds clearly suggest that the discrete nature of CF_3 "leaking" requires quantized energy input to effect detachment of each next fragment. The similarity of the said "quanta" to the gap between the large and dense groups of HOMOs and LUMOs of $C_{60}(CF_3)_{12}$ leads to the following important conclusions. Firstly, the observed fragmentation is likely to be due to the multielectron transitions. Secondly, excitation of each additional electron results in a considerable growth of detachment rates and thus increases the observed depth of detachment. These conclusions meet an important piece of support in the computationally elucidated partially σ(C–CF_3)–bonding structure of the HOMOs and partially σ*C–CF_3)-antibonding structure of LUMOs of $C_{60}(CF_3)_{12}$.

It would be appropriate to remind again that the fragmentation behavior reported herein is very similar to the sequential elimination of the C_2 units from C_{60} discussed in Refs. [1–3]. The apparent similarity between the $C_{60}(CF_3)_{12}$ and the pristine C_{60} is not only due to the similar carbon core but rather due to the highly polarizable and, perhaps, correlated shells of π electrons, which may be a key to the sufficiently high cross-sections of multielectron excitations. In this connection, investigation of the fragmentation pathways through a prism of electronic structure in a larger family of resembling molecules may be of considerable interest.

Acknowledgements

This work was performed with the partial financial support of Russian Foundation for Basic Research (grants 06-03-72007-MNTI_a, 08-02-00605-a, 08-02-97004-r_Volga region-a, 08-02-97010-r_Volga region-a). The authors are grateful to Mr. E.I. Dorozhkin for the preparation of S_6-$C_{60}(CF_3)_{12}$ sample.

References

[1] M. Foltin, M. Lezius, P. Scheier, T.D. Mark, J. Chem. Phys. 98 (1993) 9624.

[2] R. Worgotter, B. Dunser, P. Scheier, T.D. Mark, M. Foltin, C.E. Klots, J. Laskin, C. Lifshitz, J. Chem. Phys. 104 (1996) 1225.
[3] R.K. Yoo, B. Ruscic, J. Berkowitz, J. Chem. Phys. 96 (1992) 911.
[4] C.E. Klots, Z. Phys. D 21 (1991) 335.
[5] G. Gigli, S. Nunziante Cesaro, J.V. Rau, I.V. Goldt, V.Yu. Markov, A.A. Goryunkov, A.A. Popov, O.V. Boltalina, L.N. Sidorov, Fullerenes, vol. 13, Electrochemical Society Inc., 2003, p. 453.
[6] V.Yu. Markov, V.E. Aleshina, A.Ya. Borschevskiy, R.V. Khatymov, R.F. Tuktarov, A.V. Pogulay, A.L. Maximov, S.V. Kardashev, I.N. Ioffe, S.M. Avdoshenko, E.I. Dorozhkin, A.A. Goryunkov, D.V. Ignat'eva, N.I. Gruzinskaya, L.N. Sidorov, Int. J. Mass Spectrom. 251 (2006) 16.
[7] I.V. Hertel, H. Steger, J. de Vries, B. Weisser, C. Menzel, B. Kamke, W. Kamke, Phys. Rev. Lett. 68 (1992) 784.
[8] S. Hunsche, T. Starczewski, A. l'Huillier, A. Persson, C.-G. Wahlström, B. van Linden van den Heuvell, S. Svanberg, Phys. Rev. Lett. 77 (1996) 1966.
[9] N. Ju, A. Bulgac, J.W. Keller, Phys. Rev. B 48 (1993) 9071.
[10] U. Kadhane, A. Kelkar, D. Misra, A. Kumar, L.C. Tribedi, Phys. Rev. A 75 (2007), doi 041201.
[11] R.F. Tuktarov, R.F. Akhmetyanov, E.S. Shikhovtseva, Yu.A. Lebedev, V.A. Mazunov, JETP Lett. 81 (2005) 171.
[12] S.I. Troyanov, A. Dimitrov, E. Kemnitz, Angew. Chem. Int. Ed. 45 (2006) 1971.
[13] N.I. Gruzinskaya, V.E. Aleshina, A.Ya. Borschevskiy, S.I. Troyanov, L.N. Sidorov, Russ. J. Phys. Chem. 81 (2007) 312.
[14] N.A. Omelyanyuk, A.A. Goryunkov, N.B. Tamm, S.M. Avdoshenko, I.N. Ioffe, L.N. Sidorov, E. Kemnitz, S.I. Troyanov, Chem. Commun. (2007) 4794.
[15] V.A. Mazunov, P.V. Shchukin, R.V. Khatymov, M.V. Muftakhov, Mass Spectrom. 3 (2006) 11 (in Russian).
[16] NIST Chemistry Webbook, http://webbook.nist.gov/chemistry/.
[17] B. Spengler, J. Mass Spectrom. 32 (1997) 1019.
[18] A.V. Pogulay, R.R. Abzalimov, S.K. Nasibullaev, A.S. Lobach, T. Drewello, Yu.V. Vasil'ev, Int. J. Mass Spectrom. 233 (2004) 165.
[19] C. Winkler, T.D. Märk, Int. J. Mass Spectrom. Ion Proc. 133 (1994) 157.
[20] D.N. Laikov, Chem. Phys. Lett. 281 (1997) 151.
[21] I.N. Ioffe, S.M. Avdoshenko, O.V. Boltalina, L.N. Sidorov, K. Berndt, J. Weber, M. Kappers, Int. J. Mass Spectrom. 243 (2005) 223.